Award Accounts

The Chemical Society of Japan Award for Technical Development for 2005

Development of 2,2′-Iminodiethanol Selective Production Process Using Shape-Selective Pentasil-Type Zeolite Catalyst

Hideaki Tsuneki,*[1] Masaru Kirishiki,[1] and Tomoharu Oku[2]

[1]Strategic Technology Research Center, Nippon Shokubai Co., Ltd., Suita, Osaka 564-8512

[2]Strategic Technology Research Center, Nippon Shokubai Co., Ltd., Tsukuba 305-0856

Received July 26, 2006; E-mail: hideaki_tsuneki@shokubai.co.jp

Ethanolamines are produced on an industrial scale exclusively by the reaction of ethylene oxide with an aqueous solution of ammonia. The reaction is a typical consecutive reaction with three steps; therefore, it is difficult to produce 2,2′-iminodiethanol (the second product of the reaction) with high selectivity by conventional means. We developed a catalytic 2,2′-iminodiethanol selective production process using a pentasil-type zeolite catalyst modified with rare earth elements. This highly active catalyst was able to recognize the difference at molecular level between 2,2′-iminodiethanol and 2,2′,2″-nitrilotriethanol; 2,2′,2″-nitrilotriethanol was not formed in its micropore. We also succeeded in producing a binderless molded zeolite catalyst that does not form problematic impurities and that has a shape suitable for a fixed-bed reactor. The problem of activity deterioration was overcome by developing a regeneration process using high-temperature and high-density ammonia gas as a rinse medium.

1. Introduction

Ethanolamines are commodity chemicals produced at a rate of about 1.2×10^6 metric tons per year throughout the world. They are versatile chemicals that have the properties of amines and alcohols. Because of the amine functionality, they are mildly alkaline and react with acids to form salts. The alcohol functionality permits esterification and gives hygroscopic properties. Ethanolamines are used in diverse areas, such as gas sweetening, detergent and specialty cleaner formulations, intermediates for ethyleneamines, agricultural chemicals, like herbicides, urethane foam catalysts, pharmaceuticals, textile processing aids, metalworking, and oil-well rust preventatives.

Ethanolamines were prepared in 1860 by Wurtz[1] from ethylene chlorohydrin and aqueous ammonia. In 1897, an ethanolamine mixture was separated into 2-aminoethanol (MEA), 2,2′-iminodiethanol (DEA), and 2,2′,2″-nitrilotriethanol (TEA) components by Knorr by fractional distillation.[2] Ethanolamines were not available commercially before the early 1930s, and their commercial importance as intermediates started growing steadily only after 1945, because of the large-scale production of ethylene oxide (EO). The synthetic method for ethanolamines is shown in Eq. 1 to 3, which is a typical consecutive reaction with 3 steps.

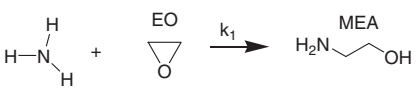

(1)

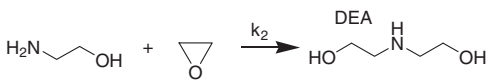

(2)

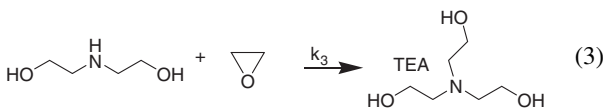

(3)

Today, ethanolamines are produced on an industrial scale exclusively by the reaction of EO with excess ammonia.[3] As pointed out by Knorr, the reaction of EO with anhydrous ammonia takes place very slowly and is accelerated by water.[4,5] The kinetics for this aqueous ammonia and EO reaction have been studied by Potter and McLaughln,[6] Lowe et al.,[7] and Miki et al.[8]

The water must be separated from the products, which is an energy-consuming disadvantage. This has led to an increasing interest in anhydrous methods using heterogeneous catalysts. Weibull et al. have reported the possibility of using ion-exchange resins. A potential disadvantage with organic ion-exchange resins is their lack of stability at high temperatures. The requirements of having high-temperature stability and of containing acidic sites are met by many inorganic solid acids, such as acidic silica–aluminas, zeolites, and acid clays.

All of the reaction steps have about the same activation energy and show a roughly quadratic dependence of the reaction rate on the water content of the ammonia–water mixture used. Therefore, product distribution depends solely on the molar ratio of ammonia to EO and not on the water content, reaction

Published on the web June 13, 2007; doi:10.1246/bcsj.80.1075

Table 1. List of Rate Constant Ratios α, β in Aqueous Ammonia Solution

	α	β	C_W/mol L^{-1}	Reference
Potter and McLaughln	6	4	18–30	6
Miki et al.	7.2–0.042C_W	16–0.22C_W	7–40	8
Ahn et al.	21.1–0.42C_W	16.4–0.25C_W		9
Park et al.	8.51–0.051C_W	14.81–0.196C_W		10
Stoyanov et al.	40	14	0.693	37
	93	81	0.411	
	105	100	0.215	
Johnson and Fred	14	40	—	38
Our results	9.36–0.153C_W	8.51–0.135C_W	6–24	This work

temperature, or pressure.[11–13] Some homogeneous catalysts, such as salts of inorganic or organic acids have been proposed by Green[14] and by Watanabe et al.[15–20] to control product distribution.

In the early 1990s, Nippon Shokubai developed a modified clay catalyst[21–24] with high activity and selectivity for MEA production, but it is very difficult to obtain DEA, which is a second-step product of a three-step consecutive reaction, selectively. In an apparent move to maximize DEA for use as an intermediate for glyphosate herbicides, Nippon Shokubai developed a process using a zeolite[25–28] to bias the product distribution towards DEA without increasing the TEA. This process was industrialized in 2003 and has operated prosperously on a scale of 50000 metric tons.

2. Conventional Aqueous Ammonia Method

2.1 Reaction Kinetics in an Aqueous Ammonia and EO System. Reaction rate (r_1, r_2, r_3) equations of each step in reaction scheme are expressed as follows:

$$r_1 = k_1 C_N C_E = d(C_M + C_D + C_T)/dt, \quad (4)$$

$$r_2 = k_2 C_M C_E = k_1 \alpha C_M C_E = d(C_D + C_T)/dt, \quad (5)$$

$$r_3 = k_3 C_D C_E = k_1 \beta C_D C_E = dC_T/dt, \quad (6)$$

where C_N, C_E, C_M, C_D, and C_T, are concentration of ammonia, EO, MEA, DEA, and TEA, respectively. k_1, k_2, and k_3 are reaction rate constants. α and β are defined as k_2/k_1 and k_3/k_1, respectively. Let C_{N0} denote $C_N + C_M + C_D + C_T$. We obtain Eqs. 7 and 8 by integration of Eqs. 4, 5, and 6.

$$\frac{C_M}{C_{N0}} = \frac{\left(\frac{C_N}{C_{N0}}\right)^{\alpha} - \frac{C_N}{C_{N0}}}{1-\alpha}. \quad (7)$$

$$\frac{C_D}{C_{N0}} = \frac{\alpha}{1-\alpha} \cdot \left[\frac{\frac{C_N}{C_{N0}} - \left(\frac{C_N}{C_{N0}}\right)^{\beta}}{1-\beta} - \frac{\left(\frac{C_N}{C_{N0}}\right)^{\alpha} - \left(\frac{C_N}{C_{N0}}\right)^{\beta}}{\alpha-\beta} \right]. \quad (8)$$

Miki et al.[8] have studied the reaction kinetics of this system and have determined the rate constants k_1, k_2, and k_3 as functions of water concentration (C_W). According to their results, k_1, k_2, and k_3 can be expressed as Eqs. 9, 10, and 11:

$$k_1 = (41 + 4.0{C_W}^2) \cdot 10^2 \cdot \exp(-11000/RT), \quad (9)$$

$$k_2 = k_1\alpha = (41 + 4.0{C_W}^2)(7.2 - 0.042C_W) \cdot 10^2 \cdot \exp(-11000/RT) = k_1(7.2 - 0.042C_W), \quad (10)$$

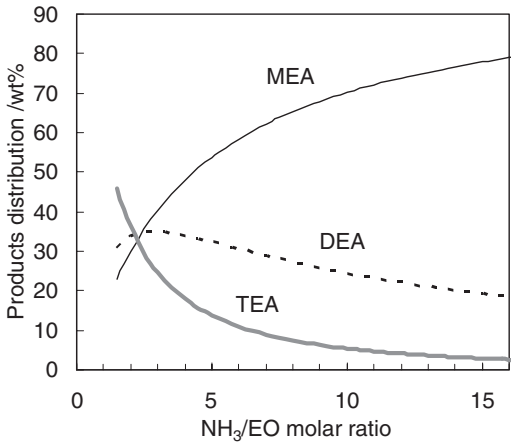

Fig. 1. Calculated product distribution as a function of molar ratio of NH_3 to EO. Reaction rate constant ratio $\alpha = \beta = 5$.

$$k_3 = k_1\beta = (41 + 4.0{C_W}^2)(16 - 0.22C_W) \cdot 10^2 \cdot \exp(-11000/RT) = k_1(16 - 0.22C_W). \quad (11)$$

They have also determined the reaction rate constants of reactions with EO and ethanolamines in anhydrous ethanolamine or high-concentration aqueous solutions of ethanolamine at 303 K.

$$k_2' = (6.6 + 6.0{C_W}^{1/2}) \cdot 10^{-3}. \quad (12)$$

$$k_3' = (16 + 3.1{C_W}^{1/2}) \cdot 10^{-3}. \quad (13)$$

Equation 12 or 13 is very different from Eq. 10 or 11. It is thought that the hydroxy group of ethanolamines has catalytic activity like water.

Table 1 shows the reaction constant ratios that we and other researchers have determined. Solving Eqs. 7 and 8 numerically, these parameters (α, β) have been calculated from product distribution. Selectivity for MEA increases when these parameters diminish. We also obtained similar results. In the industrially operable range of water concentration, α and β were about 5–7. Figure 1 shows calculated product distribution of the reactants in the case of $\alpha = \beta = 5$ as a function of NH_3/EO molar ratio. In the most efficient condition (NH_3/EO = 2–4), three components were formed in similar quantity. A high NH_3/EO ratio was required to obtain a high MEA yield, and then large amounts of ammonia and water had to be recycled.

Table 2. Rate Constant Ratios of Various Homogeneous Catalysts in Aqueous Ammonia

Catalyst	Catalyst /wt %	Water content /wt %	EO content /wt %	NH_3 content /wt %	NH_3/EO molar ratio	α	β
$(NH_4)_2CO_3$[a)]	32.6	40.4	15.7	22.9	3.77	ca. 2	—
$(NH_4)_2CO_3$	21.4	55.6	13.0	11.3	3.52	1.37	4.06
	22.6	36.2	20.8	16.1	3.54	1.96	4.68
NH_4Cl	33.3	49.3	11.7	18.5	3.60	2.68	4.34
NH_4NO_3	35.1	40.7	8.8	14.3	3.83	2.89	4.91
$(NH_4)_2SO_4$	35.1	40.2	10.5	15.8	3.46	3.47	8.39
NH_4Br	35.1	40.7	8.8	12.8	3.83	2.48	4.01
$ClCH_2COONH_4$	16.9	62.2	10.0	15.1	3.50	2.71	4.18
	25.4	55.0	10.0	15.1	3.50	2.48	4.27
	33.7	47.9	10.0	15.1	3.50	2.18	4.56
CH_3COONH_4	30.0	51.7	10.4	16.0	3.52	3.35	4.20
$HCOONH_4$	14.3	66.0	10.0	15.1	3.48	3.76	4.75
$CH_3CH(OH)COONH_4$	27.7	49.8	11.4	14.0	3.49	3.42	4.69

a) Reynhart[33] MEA yield: 66.2 wt %, other data based on Watanabe et al.[15–17]

2.2 Process Description of a Conventional Aqueous Ammonia Process. In a conventional process, the reaction takes place in liquid phase, and the operation pressure must be sufficiently large to prevent vaporization of ammonia at the reaction temperature. In current procedures, the pressures are up to 15 MPa, the reaction temperatures are up to 420 K, and an excess up to 40 mol of ammonia per 1 mole of EO is used. The reaction is highly exothermic; the heat of reaction is about 125 kJ per mole of EO. Unreacted ammonia and water, fed in as a catalyst, are separated from the end products in a distillation line downstream of the reactor, and are recycled. In large-scale continuous single-line plants, the requirement for low energy use (i.e., operation with minimum steam consumption) determines both the transport of heat from the reactor and the design of the thermally integrated distillation line. The ethanolamine mixture is worked up in vacuum distillation columns to give pure products.

Product distribution of the three ethanolamines can be controlled by an appropriate choice of the ammonia to EO ratio, as shown in Fig. 1. A higher DEA or TEA content can also be obtained by recycling MEA or DEA to the reactor or by reacting them with ethylene oxide in a separate unit. Several improved processes have been proposed by some producers.[29,30] Gibson et al.[31,32] have shown that a high MEA yield is obtained in very low water content when the reaction is carried out in supercritical condition. For example, if C_W is 1.02 mol L^{-1} (i.e., the water concentration equals 2.84 wt %), the NH_3/EO ratio is 44, reaction temperature is 347 K, and the reaction pressure is 20.7 MPa, the product mixture had the following composition: MEA: 83 wt %, DEA: 15 wt %, TEA: 2 wt %. The disadvantage of this process is the high equipment cost due to the high reaction temperature and pressure.

3. Homogeneous Catalyst

Some attempts have been made to avoid the disadvantage of the aqueous ammonia system using a homogeneous catalyst. Reynhart has revealed that ethanolamines can be produced from ammonia or a primary amine and ethylene oxide, and a salt of a weak acid, such as ammonium carbonate.[33] Watanabe et al.[15–17] have proposed ammonium salts, such as carbonate, nitrate, chloride, sulfate, and carboxylate. Rate-constant ratios of these catalysts are shown in Table 2. They have also developed a process using these catalysts, such as the recovery of the catalyst (as CO_2), purification by distillation, and MEA or DEA recycle.[18–20] In the case of ammonium monochloroacetate, α values decrease (i.e., MEA selectivity increases) along with an increase of the amount of catalyst. Ammonium carbonate has especially excellent MEA selectivity, but in spite of an improvement in the α, β values, they did not decrease markedly. In addition, this homogeneous catalyst system required a large amount of catalyst (catalyst to EO molar ratio 0.5–2.4) and water.

Table 3. Rate Constant Ratios of Various Homogeneous Catalysts in Anhydrous System

Catalyst	Concentration /mol L^{-1}	Content /wt %	α	β
Water (control)	6.14	17.2	8.81	8.08
NH_4Cl	0.97	8.4	8.56	7.42
	3.22	24.8	6.00	5.76
CH_3COONH_4	1.0	7.8	8.3	8.6
	3.0	23.4	7.7	6.1

We examined the catalytic properties of ammonium salts in anhydrous systems. Ammonium chloride and acetate indicated catalytic activity, and their α and β values are listed in Table 3. The behavior of β was similar to α, contrary to Watanabe's results. However, for practical use, this system also required a large amount of catalyst, and catalyst recovery was very difficult and uneconomical.

4. Heterogeneous Catalyst for MEA Selective Production

4.1 Ion-Exchange Resin. Product distribution is controlled by the NH_3/EO ratio in the reaction mixture. If an MEA-rich composition is desired, the reaction must be carried out with a greater NH_3/EO ratio. When a conventional aqueous ammonia method is used, a large amount of water as well as unreacted ammonia must be recycled. Water has a very large latent heat of vaporization, and thus, an anhydrous reaction system has been desired. In the 1950s, Weibull described the reaction of

Table 4. Catalytic Performance of Cation-Exchange Resin[35 a)]

NH_3/EO molar ratio	Reaction temperature /K	Reaction pressure /MPa	WHSV /g gcat^{-1} h^{-1}	Product distribution/wt %			α	β
				MEA	DEA	TEA		
40	353[b)]	8.1	10	89.5	9.9	0.6	5.50	5.27
	373[b)]	10.1	13	89.4	10.1	0.5	5.58	4.32
	393[b)]	12.2	14	85.8	12.7	1.5	7.77	10.39
	413[b)]	14.7	25	84.3	14.1	1.6	8.81	10.07
21	318–385[c)]	11.1	—	84.2	14.7	1.1	4.63	3.46
44	328–383[c)]	11.1	—	91.0	8.6	0.4	5.09	4.43

a) EO conversion > 99 mol %. b) Isothermal condition. c) Adiabatic condition.

alkylene oxides and ammonia in an anhydrous batch-wise reaction system,[34] using cation-exchange resins saturated with hydrogen or non-quaternary ammonium ions and anion-exchange resins partly or fully saturated with organic or inorganic acids as catalysts. In 1968, Weibull et al. proposed a continuous system using cation-exchange resins[35] as the heterogeneous catalyst for an anhydrous NH_3/EO reaction. They list many types of cation-exchange resins with active groups like sulfonic, carboxylic, and phosphoric acid groups; basic resins: polystyrene, copolymers of styrene, and divinylbenzene, polymethacrylic acid, and processed coal. In their example, a commercially available sulfonated styrene–divinylbenzene copolymer strong acid-type resin has been used. The reaction is carried out under elevated pressures (8–14.5 MPa) and reaction temperatures (298–413 K) using a fixed-bed-type reactor. The reaction can be carried out under isothermal or adiabatic conditions. Under isothermal conditions, the preferred reaction temperature range is 348–410 K. Since the reaction is strongly exothermic, it is necessary to eliminate reaction heat from the reaction mixture to keep the temperature approximately constant. It is generally preferable to carry out the reaction under adiabatic or nearly adiabatic conditions, because no cooling equipment is required. In this case, the reactants are preheated to 298–348 K before they are introduced into the reactor. Because of the reaction heat evolved, the reaction temperature is rapidly increased. The maximum reaction temperature may not be obtained until the mixture has reached the end of the catalyst bed. Table 4 shows reaction conditions, product distribution and kinetic parameters (α, β). MEA selectivity, which is represented by α and β, of the ion-exchange resin is similar to aqueous ammonia systems.

Kamemski et al.[36] and Stoyanov et al.[37] have studied the catalytic reaction of EO and anhydrous ammonia using an ion-exchange resin catalyst (wofatit kps-H^+). This resin is a more effective catalyst than water (10 g-ion/L of kps have the same activity as 10 to 15 wt % water). They have derived the kinetic model for this consecutive reaction at 323–352 K. According to their study, the conversion of DEA to TEA has a fractional order (0.25) in DEA, but all other reactions are first order in each reactant. In addition, a DEA formation path directly from ammonia and EO has been proposed.

4.2 Inorganic Solid Acid Catalyst. The process using the cation-exchange resin has been commercialized. However, organic resin catalysts are not as stable in high-temperature situations as is desired. Therefore, a more stable and more selective catalyst is required. Johnson et al.[38] have proposed inorganic acid compounds, such as acidic silica–aluminas, zeolites, molecular sieves, acid clays, or other acid metal oxides. The preferred catalysts are the silica–aluminas, also known as aluminosilicates. These catalysts typically contain a proportion of aluminum oxide. Grice and Knifton[39] have proposed an acidic clay obtained by treating montmorillonite with heteropolyacid (e.g., 12-tungstophosphoric acid, 12-tungstosilicic acid, or 12-molybdophosphoric acid), or with group 3 or 13 metal chlorides (e.g., $TiCl_4$, $ZrCl_4$, or $AlCl_3$). Vamling and Cider[40] have discussed the ability of different forms of zeolites to catalyze the formation of MEA, DEA, and TEA from EO and ammonia in the liquid phase, as well as a comparison of zeolite catalysts with organic ion-exchange resins. They have predicted the product distribution and the capacity of a full-scale adiabatic packed-bed reactor for the different catalysts. They have adapted a simple second-order consecutive reaction model and built up a reactor math model for scale-up. Table 5 shows the catalyst, NH_3/EO ratio, product distribution, and kinetic parameters (α, β). The α values in Table 5 are less than those in Table 4. These inorganic catalysts can be expected to be more stable in high temperatures, but their catalytic performances do not match that of the organic resin.

Decker et al.[41–44] have reported the vapor-phase reaction of EO and ammonia using various solid catalysts. Table 6 shows their results with various catalysts. Catalytic activities of these catalysts in vapor-phase reaction were quite low (EO conversion: 20–30 mol %), and their MEA selectivity is extremely low (α value: 30–300). In addition to these disadvantages, considerable side reactions occur, and large amounts of byproducts (10–60 wt %) form.

4.3 Clay Catalyst Modified with Rare Earth Element. 4.3.1 Catalyst Screening: As mentioned above, past inorganic acid catalysts do not have enough performance for MEA selective production. We started development of various catalysts without limiting solid acid catalysts, such as heteropolyacid (Cs acid salt and multivalent metal salts), phosphoric acid salts (α-zirconium phosphate, γ-zirconium phosphate, and boron phosphate), oxides or mixed oxides (silica–alumina, titania–silica, titania–zirconia, and activated alumina), magic acid (nafion and SO_4/ZrO_2), metal sulfates, solid base (magnesia and hydrotalcite), layered clays (montmorillonite and saponite), and zeolite. Figure 2 shows the laboratory scale equipment used in our experiments. When a heat-exchanger-type reactor was used, unreacted EO concentration was measured using an online gas chromatograph. On the other hand, when an adiabatic reactor was used, unreacted EO was scarcely

Table 5. Catalytic Performance of Various Inorganic Acid Catalysts in Liquid-Phase Reaction

	Catalyst	NH_3/EO molar ratio	Pressure /MPa	Temperature /K	LHSV /g h^{-1} cm^{-3}	EO conv. /mol %	Product distribution/wt %			α	β
							MEA	DEA	TEA		
Johnson and Fred[38]	Silica–alumina	39.88	10.1	383	0.97	98	87.04	10.12	2.10	6.54	18.2
	Molecular sieves AW500	17.65	10.8	398	1.79	98	74.68	22.01	3.27	7.31	6.12
Grice and Knifton[39]	Acid-activated clay	19.4	17.3	413	14.8	99	75.7	20.0	4.0	7.87	8.88
	PW_{12}/clay	26.4	20.7	423	9.0	92.6	82.5	14.3	2.7	6.65	11.51
	$TiCl_4$/clay	19.6	17.3	413	15.8	92.5	69.4	22.3	7.2	10.80	15.87
Vamling and Cider[40]	Molecular sieves 13X	20–31	13.6	328–358	13.5–19.2	99–100				13.5 ± 1.1	9.4 ± 8.2
	Molecular sieves AW500	20–37	13.7	371–400	8.5–13.0	72–84				6.03 ± 0.23	7.8 ± 0.48
	Y-Zeolite	30–42	13.3	355–378	12.5–20	84–99				10.7 ± 0.72	15.9 ± 10.0

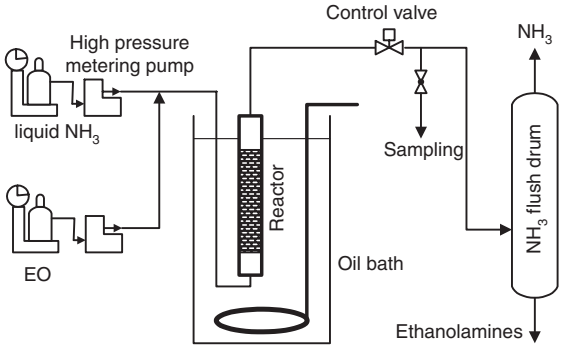

Fig. 2. Laboratory scale experimental equipment. Reactor: 10.7 mm$^{\phi}$ × 250 mm^{L}, catalyst: 5–10 g, heat-exchange-type reactor: bath temp: 340–400 K, adiabatic-type reactor: reactor inlet temp: 320–350 K, reaction pressure: 12–14 MPa, NH_3/EO molar ratio: 5–15, WHSV: 5–15 g gcat^{-1} h^{-1}.

detected (EO conversion of about 100%). The catalysts that show significant high activity worthy to measure MEA selectivity were silica-supported heteropoly iron salts, slica–alumina, layered clay, and pentasil-type zeolite (e.g., ZSM-5, ZSM-11). Table 7 shows the catalytic performances of these catalysts. In particular, layered clays, such as montmorillonite or saponite, showed high MEA selectivity comparable to ion-exchange resin.

4.3.2 Control of Catalyst Acid–Base Properties: Acid properties of these catalysts were controlled to improve their activity and selectivity. Silica–alumina, which is treated with a base, does not have a strong acidic site. Therefore, catalytic activity was not expected in a reaction catalyzed by a strong acid site. However, as shown in Table 7, silica–alumina impregnated with NaOH (see Entry 2) had greater activity and selectivity than non-treated silica–alumina (see Entry 1). This means that an active site effective for the reaction may not be always be a strong acid site. Then, acid catalysts were modified with various metal elements (Cu, Ni, Zn, Mg, Ca, Sr, Ba, Al, Fe, La, Y, Yb, and Ce) by ion-exchange methods, or by impregnation, in order to control their acid–base properties. As shown in Entries 3, 6, 9, 10, and 12 of Table 7, the activities of catalysts modified with rare earth elements were improved as compared with others. Silica–yttrium catalyst (see Entry 4), which is a weak-base catalyst, showed considerable activity.

In order to prepare a heat-resistant catalyst, it is necessary to calcine the catalyst at a high temperature. When the inter-layer cation in clay is exchanged by a multivalent metal cation, the hydrated metal cation becomes a strong acid site.[45] Therefore, if cation-exchanged clay is treated in a temperature high enough to lose water, a strong acid site, formed with hydrated cation, is also lost. However, if an active catalyst does not need a strong acid site, the cation-exchanged layered-clay catalyst can be calcined at temperatures above 400 K. Table 8 shows the effect of the calcination temperature of layered-clay modified with a rare earth element. The activity and selectivity improved as the calcination temperature increased. Figure 3 shows the crystal structure of layered-clay at various calcination temperatures. XRD analysis showed that the layer structure was destroyed as the calcination temperature increased.

Table 6. Catalytic Performance of Various Catalysts in Vapor-Phase Reaction[41–44]

Catalyst[a)]	NH_3/EO molar ratio	Reaction temp/K	GHSV /h^{-1}	EO conv/%	Product distribution/wt %				α	β
					MEA	DEA	TEA	others		
Active carbon[41]	6	463	400	25	24	15	34	27	88	195
Al_2O_3[41]	8	363	200	10	25	10	5	60	149	243
Silica–alumina[41]	10	463	200	47	42.1	7.2	46.3	4.4	37	342
Zeolite 13X[42]	5	333	300	22	38	18	17	27	36	73
Faujasite zeolite[43]	6	363	400	30	36.4	8.1	39.5	16	38	266
Pentasil zeolite[44]	6	333	400	30	9	55	23	13	253	29

a) Catalyst 5 cm^3.

Table 7. Activity and Selectivity of Various Catalysts in Liquid-Phase Reaction[a)]

Entry	Catalyst	WHSV /g gcat^{-1} h^{-1}	Bath temp /K	EO conversion /mol %	α	β	$\gamma = \alpha/\beta$
Ref.	Cation-exchange resin (Dowex-50W)	14.3	361	97.7	5.5	4.9	1.1
1	SiO_2–Al_2O_3	6.3	380	92.2	9.2	14.0	0.7
2	SiO_2–Al_2O_3–Na_2O	6.2	381	96.0	6.8	8.8	0.8
3	SiO_2–Al_2O_3–Y_2O_3	10.0	373	98.0	7.6	12.0	0.6
4	SiO_2–Y_2O_3	11.5	389	97.6	7.0	8.2	0.9
5	H-ZSM-5	10.4	384	91.2	7.7	6.5	1.2
6	La-ZSM-5	12.1	359	97.0	8.6	2.4	3.6
7	H-montmorillonite	10.1	384	92.0	5.4	4.2	1.3
8	Na-montmorillonite	14.5	391	88.9	5.7	5.4	1.1
9	La-montmorillonite	10.0	360	98.1	5.0	3.7	1.4
10	Y-montmorillonite	11.2	360	97.6	4.3	2.8	1.5
11	H-saponite	9.9	360	94.5	5.8	4.3	1.3
12	La-saponite	10.6	353	93.9	5.3	4.6	1.2

a) Heat-exchanger-type reactor, inner diameter 10.7 mm^{ϕ}, NH_3/EO molar ratio 10 to 17, reaction pressure 12 to 14 MPa, oil bath temperature 360 to 390 K, WHSV 5 to 15 g gcat^{-1} h^{-1}. $\alpha = k_2/k_1$: indicator of MEA selectivity (the smaller the better). $\gamma = k_2/k_3 = \alpha/\beta$: indicator of DEA selectivity (the larger the better).

Table 8. Effect of Calcination Temperature of Clay Catalyst on Activity and MEA Selectivity[a)]

Entry	Calcination temperature /K	Oil bath temp /K	EO conv /mol %	α	β
1	393	363	95.4	4.9	3.9
2	573	370	96.8	4.1	3.4
3	673	367	93.6	3.6	4.2
4	773	361	96.0	3.4	3.0

a) Catalyst: Layered-clay modified with rare earth element. NH_3/EO molar ratio: 10 to 12, WHSV: ca. 11 g gcat^{-1} h^{-1}.

The layer structure of the catalyst calcined at 773 K collapsed completely. This means that the active sites are not inter-layer hydrated cations but are rare earth element cations fixed on surface ion-exchange site.

4.3.3 Reactant Diffusion Effect on Activity and Selectivity: A particle diameter effect on activity at replication examination of ion-exchange resins was observed. Reactant diffusion possibly affects the apparent catalytic activity and selectivity in the case of fast reaction in a liquid phase, such as the catalytic EO/NH_3 reaction. In the case of layered-clay catalyst modified with a rare earth element and calcined at 773 K, the catalyst particle diameter effect on activity and selectivity

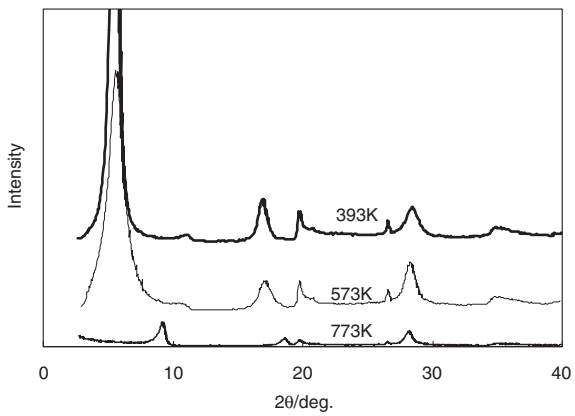

Fig. 3. XRD pattern of layered-clay calcined on various temperatures Cu Kα.

was investigated. Table 9 shows the EO conversion of catalysts of various sizes. The EO conversion of relatively large-diameter catalysts (see Entry 3) was quite low even if the reaction temperature was 14 K higher than the standard condition. The activity of the Entry 3 catalyst was much smaller than that of the Entry 1 catalyst. This means that a large-diameter catalyst does not work effectively by limitation of the reactant diffusion rate, that is, the catalyst effectiveness factor is

Table 9. Effect of Particle Size of Catalyst Pellet on Apparent Activity[a)]

Entry	Particle size /mm	Oil bath temperature/K	EO conv. /mol %	α	β
1	0.149–0.297	363	95.4	4.3	4.0
2	0.65–0.35	372	92.8	4.6	4.3
3	0.71–1.0	387	87.6	5.8	5.4

a) Catalyst: Layered-clay modified with rare earth element calcined at 773 K. NH_3/EO molar ratio: 10 to 12, WHSV: ca. 11 g gcat^{-1} h^{-1}.

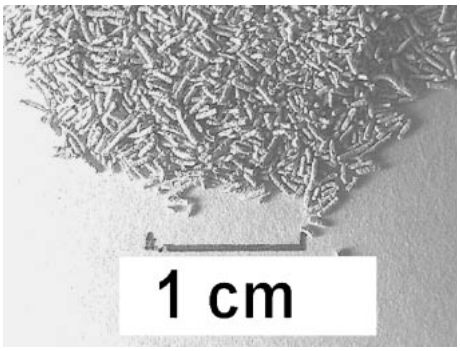

Fig. 4. An example of molded layered clay catalyst.

Table 10. Impact of Pore Volume of Catalyst on Apparent Activity[a)]

Entry	Pore volume /cm^3 gcat^{-1}	Particle size /mm	Oil bath temperature/K	EO conv /mol %	α	β
1[b)]	0.08	0.7–1.0	387	87.6	5.8	5.4
2[b)]	0.26	0.7–1.0	378	96.8	4.8	4.3
3[b)]	0.39	0.7–1.0	373	97.4	4.0	3.8
4[c)]	0.38	$0.3–0.4^{\phi} \times 2–5^{L}$	363	94.1	3.1	3.0

a) Catalyst: Layered-clay modified with rare earth element calcined at 773 K. NH_3/EO molar ratio: 10 to 12, WHSV: ca. 11 g gcat^{-1} h^{-1}. b) Pulverized type. c) Extruded type.

much smaller than unity.

The catalyst effectiveness factor η is a function of Thiele modulus[46] ϕ. In the case of spherical particles, this function is expressed as

$$\eta = \frac{3}{\phi}\left(\frac{1}{\tanh(\phi)} - \frac{1}{\phi}\right). \quad (14)$$

Thiele modulus ϕ is defined as

$$\phi = R\sqrt{\frac{k}{D_{\text{eff}}}} = R\sqrt{\frac{k}{D\theta/\tau}} \quad (15)$$

k: Reaction rate constant, D_{eff}: effective diffusion coefficient ($=D\theta/\tau$), D: diffusion coefficient, θ: pore ratio (=pore-volume/catalyst particle volume), τ: tortuosity factor, R: catalyst particle radius. It is effective to enlarge the effective diffusion coefficient in order to enlarge the catalyst effectiveness factor. Increasing the pore ratio tends to decrease the tortuosity factor. It is very effective to enlarge the pore ratio. A large pore-volume catalyst is prepared by the following procedure: (1) add a pore-forming agent to a precursor and mix them well, (2) mold the mixed material to a pellet, and (3) calcine the pellet at high temperatures to remove a pore-forming agent by decomposition or by combustion.

These pore-forming agents include, for example, various ammonium salts, such as ammonium nitrate and ammonium acetate, organic compounds, such as urea, and various polymers and fibers. Water-insoluble organic compounds can be used in view of their efficiency of pore formation and ease of molding. Figure 4 shows an example of a molded layered clay catalyst. The pellet diameter (correspond to R in Eq. 15) was very small in order to decrease diffusion distance. Table 10 lists the EO conversion of various pore-volume catalysts. The apparent activities of the catalysts markedly increased as the pore volume increased. This means that a large pore-volume catalyst has a large effective diffusion coefficient and a large catalyst effective factor.

Similarly, the diffusion of the reactants and products affects selectivity. In the case of the ion-exchange resin, α of 50–100 mesh-sized (0.075–0.150 mm) resin was about 5, while that of 20–50 mesh-sized (0.15–0.8 mm) resin was 6–7. In the case of a layered-clay catalyst modified with a rare earth element, α of a standard catalyst (about 0.2 mm in diameter) was about 3, while that of a large particle size catalyst (about 2–3 mm) was 6–7. This reaction is a typical consecutive reaction (MEA $\rightarrow$ DEA $\rightarrow$ TEA). Therefore, in a region where effect diffusion cannot be ignored, the second or third reaction preferably occurs according to a longer residence time[47] in the catalyst pellet.

Figure 5 shows the MEA concentration in a reactant mixture in the case of an ion-exchange resin and a layered-clay catalyst modified with a rare earth element. Selectivity-improved layer-clay catalysts required only about half the NH_3/EO ratio compared with ion-exchange resin.

5. Heterogeneous Catalyst for DEA-Selective Production

Recently, the demand for DEA as an intermediate for glyphosate herbicides has markedly increased. Product distribution could be controlled by NH_3/EO ratios as shown in Fig. 1. DEA fraction was only 35 wt % at most. If a part of the formed MEA is recycled to the reaction mixture, the net DEA fraction may increase, but it has a limitation. Figure 6 shows the calculated net product distribution when a part of the MEA was recycled to the reaction mixture when the (NH_3 + MEA) to EO molar ratio was 8. Even when equal amounts of MEA to produced DEA was recycled, the DEA fraction was only 43 wt %, and the TEA fraction reached 14 wt %. Therefore, a high DEA-selective catalyst is necessary

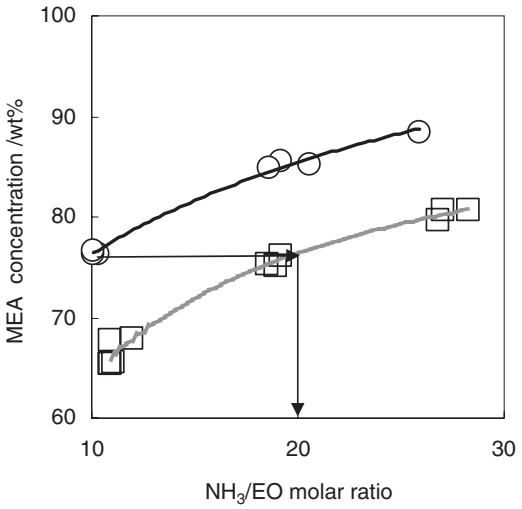

Fig. 5. MEA concentration in produced amines as a function of molar ratio of ammonia to EO. ○: Layered-clay modified with rare earth element 0.3–0.4 mm^{ϕ} × 2–5 mm^{L}, □: Dowex-50W 20–50 mesh (0.3–0.8 mm).

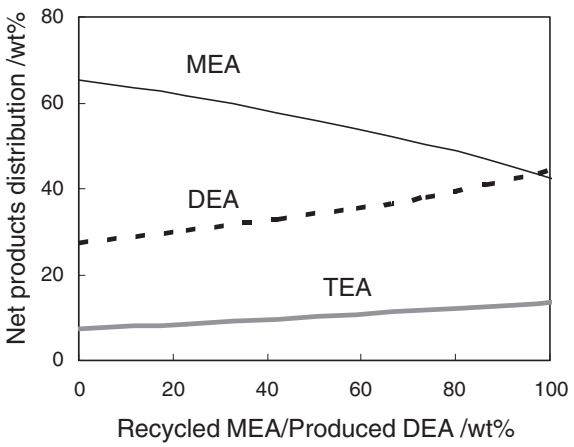

Fig. 6. Calculated net product distribution when MEA recycled in conventional process. $(NH_3 + MEA)/EO$ ratio = 8, $\alpha = \beta = 5$.

so that formation of TEA is restrained and formation of DEA is increased.

5.1 Molecular Recognition Ability of Zeolite. The molecular diameter of a branched molecule (TEA) is 1 nm and that of a straight molecule (MEA and DEA) is 0.47–0.49 nm. There is a significant difference between the sizes of these molecules. The concept of molecular sieves is the separation technology utilization of this difference between sizes in molecular order. The micro-reaction field in a zeolite micropore can be effective for selective DEA formation if the zeolite is able to recognize the difference between ethanolamines. Figure 7 shows the pentasil-type zeolite framework structure and molecular structure of ethanolamines. DEA, having small molecular diameter, is able to enter the zeolite micropore, but TEA, having a branching structure, is not. Adsorption examinations of MEA and TEA to various zeolites were made to confirm this expectation. Table 11 shows the saturated adsorption amount of ethanolamines (MEA and TEA) to various zeolites. Adsorption

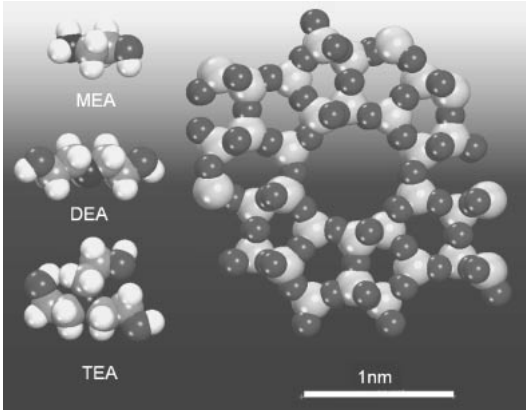

Fig. 7. Pentasil-type zeolite frame work structure and molecular structure of ethanolamines.

Table 11. Ethanolamines Adsorption to Various Zeolites in Aqueous Solution

Catalyst	Adsorbed MEA /meq g^{-1}	Adsorbed TEA /meq g^{-1}	MEA /TEA
Ion-exchange resin Dowex 50W	5.18	4.95	1.05
H-Y-zeolite	2.33	2.08	1.12
H-Mordenite	2.13	0.89	2.39
H-L-zeolite	2.35	1.24	1.90
H-ZSM-5	0.60	0.10	6.00

amount of MEA or TEA to ion-exchange resin, having no micropore, was nearly equal to its exchange capacity. No difference between MEA and TEA was observed. The ratio of the adsorption amount of MEA and TEA was varied with the zeolite micropore structure. The ratio in Y-zeolite that has a relatively large pore was close to unity. The ratio in mordenite or L-zeolite was markedly larger than unity. In the case of ZSM-5, having a small pore diameter (0.55 nm) close to the MEA molecular diameter (0.47 nm), the ratio of the adsorption amount of MEA and TEA was very large (6). This means that ZSM-5 can recognize the difference between MEA and TEA.

5.2 Implementation of Shape Selectivity. There are three possible types of restriction in shape selectivity:[48] (1) reactant restriction, (2) product restriction, and (3) transition-state restriction. DEA-selective catalysts must have shape selectivity by transition-state restriction. Figure 8 shows the reaction model in zeolite micropores. An MEA molecule can react with EO to form DEA in a narrow micropore, but DEA cannot react with EO to form TEA by transition-state restriction. ZSM-5, which can recognize the difference between MEA and TEA, is expected to realize this shape selectivity. Reaction data of H-ZSM-5 is shown in Table 7, Entry 5. Against expectations, H-ZSM-5 showed comparatively low activity and a low DEA selectivity indicator γ (1.2). On the other hand, La-ZSM-5 (see Entry 6), which was prepared by La ion exchange, showed high activity and comparatively high γ (3.6). Table 12 shows the effect of lanthanide-ion-exchange amount to DEA selectivity. Along with lanthanide-ion-exchange amount, β decreased significantly, that is, formation of TEA was depressed. In addition, γ drastically increased up to 50. The reason why mere

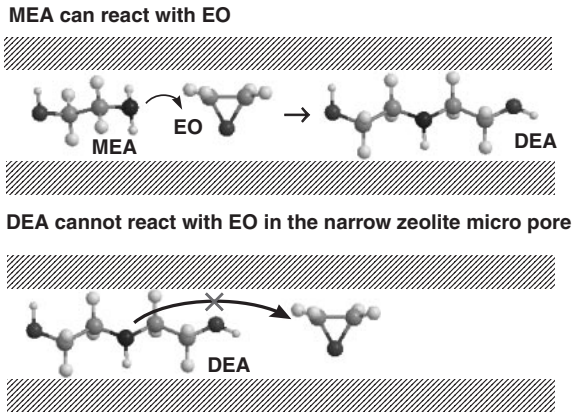

Fig. 8. Reaction model in the zeolite micro pore.

Table 12. Impact of Lanthanide-Ion-Exchange Amount on DEA Selectivity[a)]

Entry	La/Al atomic ratio	Time on stream/h	α	β	γ
1	0.017	2	7.81	0.61	12.8
		24	7.69	1.53	5.0
2	0.1	2	8.47	0.21	39.9
		24	8.33	0.59	14.1
3	0.12	2	8.70	0.20	50.1
		24	8.26	0.56	14.7

a) Catalyst: ZSM-5 Si/Al = 28. Reaction condition 10 mm$^{\phi}$ adiabatic reactor, NH_3/EO molar ratio 15. Reaction pressure 12 MPa, WHSV 10 g gcat^{-1} h^{-1}. Reactor inlet temperature 343 K, EO conversion about 100%.

H-ZSM-5 does not show DEA selectivity is that a non-selective self-catalytic reaction by the hydroxy group of ethanolamines occurs significantly, because of its low activity, and this cancels its shape selectivity.

Reaction rate constants k_1, k_2, and k_3 in Eqs. 4, 5, and 6 are considered as follows:
C_O is the concentration of the hydroxy group defined as $C_M + 2C_D + 3C_T$

$$k_1 = k_{1c} + k_{1nc} + k_O C_O, \quad (16)$$

$$k_2 = k_1\alpha = k_{1c}\alpha_c + k_{1nc}\alpha_{nc} + \alpha_O k_O C_O, \quad (17)$$

$$k_3 = k_1\beta = k_{1c}\beta_c + k_{1nc}\beta_{nc} + \beta_O k_O C_O, \quad (18)$$

$$\alpha = (k_{1c}\alpha_c + k_{1nc}\alpha_{nc} + \alpha_O k_O C_O)/(k_{1c} + k_{1nc} + k_O C_O), \quad (19)$$

$$\beta = (k_{1c}\beta_c + k_{1nc}\beta_{nc} + \beta_O k_O C_O)/(k_{1c} + k_{1nc} + k_O C_O), \quad (20)$$

$$\gamma = (k_{1c}\alpha_c + k_{1nc}\alpha_{nc} + \alpha_O k_O C_O) / (k_{1c}\beta_c + k_{1nc}\beta_{nc} + \beta_O k_O C_O). \quad (21)$$

The subscripts c, nc, and O of each parameter denote intrinsic catalytic, non-catalytic, and self-catalytic (OH), respectively. If k_{1c} (reaction rate constant of a catalyst) is much smaller than k_O (reaction rate constant of self-catalytic reaction), then the apparent γ value is far from the true value. Figure 9A shows tangible product distribution (the right axial scale is 10 times that of the left). The DEA fraction at the same NH_3/EO molar ratio was larger than that of Fig. 1 (aqueous NH_3 method) and, at the same time, the TEA fraction was extremely small. This result reveals that this catalyst has shape selectivity.

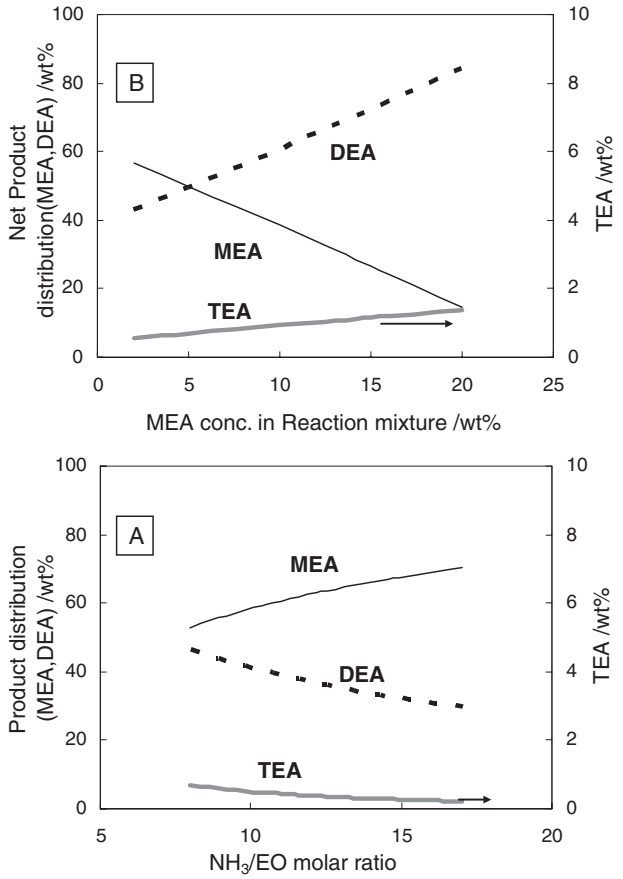

Fig. 9. Initial catalytic performance. A: impact of NH_3/EO molar ratio, B: impact of MEA concentration in reaction mixture (NH_3/EO = 10). Catalyst La-ZSM-5, reaction pressure 10 MPa, WHSV 10 h^{-1}.

Figure 9B shows the net product distribution of ethanolamines when a part of produced MEA is recycled to the reaction mixture. When the MEA concentration in the reaction mixture was 10 wt % (recycled MEA/produced DEA ratio: 70%), the DEA fraction reached more than 60 wt %, and the TEA fraction was only 0.9 wt %. The DEA fraction of Fig. 9B by comparison with that of Fig. 6 shows that the MEA recycle effect of the DEA-selective process is much larger than that of a conventional process.

A multivalent metal cation, such as lanthanide, is strongly hydrated in aqueous solution, and its hydrated ion diameter is large. It is difficult to exchange a small cation in the narrow micropore of ZSM-5 with a large cation. Therefore, the ion-exchange amount of a catalyst that is prepared by ion-exchange operation in an aqueous solution was small (Entry 1 in Table 5). Jia et al.[49] and Rauscher et al.[50] have suggested that the ion-exchange amount of zeolite can be improved by a solid-state process. It seems that a bare cation is relatively small and can diffuse easily into the micropore of the zeolite at high temperatures, above 700 K. The following experiment was executed to reveal that ion exchange can occur in solid state. First, a mechanical mixture of $LaCl_3$ and NH_4-ZSM-5 (Si/Al ratio: 28) was carefully ground in a mortar for several minutes. The La/Al atomic ratio in the mechanical mixture was 0.114. The ground mixture was then transferred to a por-

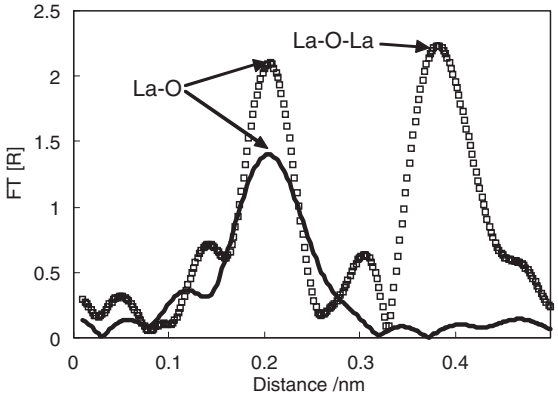

Fig. 10. La K-edge FT-EXAFS spectra (SPring 8 BL19B2). □: La_2O_3, solid line: La-ZSM-5.

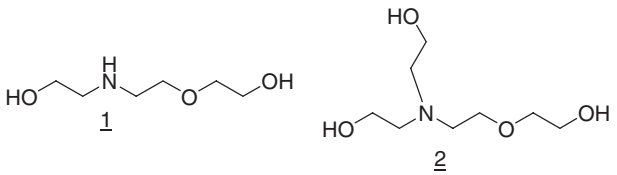

Fig. 11. Impurities formed by binder-containing zeolite.

celain dish and calcined in a muffle furnace at 823 K for 5 h. The resulting sample was washed four times with deionized water. It was finally dried overnight at 393 K. The La/Al atomic ratio in the final sample, determined by ICP analysis, was 0.11. The catalysts in Table 12 were prepared by a solid-state ion-exchange procedure adopting this concept.[51]

Figure 10 shows La K-edge FT-EXAFS spectra of La-ZSM-5 compared with La_2O_3. The peak assigned as La–O–La existed in La oxide spectra, but this peak was not observed in La-ZSM5 spectra. This suggests that La ion in ZSM-5 is isolated and is fixed to an ion-exchange site without aggregation to form oxide.[52]

5.3 Development of Molded Binderless Zeolite. Generally, a high silica zeolite, such as pentasil-type zeolite, has poor plasticity and formability. Therefore, it is very difficult to mold without an inorganic binder. A commercially available molded zeolite usually contains 20 to 40 wt % binder, such as alumina. Impurities (1 and 2 in Fig. 11) were formed using a catalyst made of a binder-containing zeolite. Entry 1 of Table 13 shows an example of impurities contents, and Entry 2 shows that no impurities are formed by the zeolite without binder. It seems that the impurities are formed on the basic-site of binder. Boiling points of these impurities were high and close to the boiling point of TEA. The temperature of the distillation column must be low to prevent coloring. The distillation column must be operated in a very high vacuum, such as 100 to 300 Pa, and its pressure drop must be very small. To reduce its pressure drop, the (packed) height of the column must be low. It is difficult to separate them from TEA using such a low-distillation column because of the separation ability shortage. The formation of these glycol ether-type impurities has been encountered in conventional aqueous ammonia methods. Washington et al.[53,54] have proposed adding carbon dioxide to the reaction mixture in order to reduce these impurities. Adding carbon dioxide is not preferred in an anhydrous system.[55]

Table 13. Content of Impurities Formed by Binder-Containing Zeolite[a)]

Entry	Catalyst[b)]	Content/wt %				
		MEA	DEA	TEA	Impurity 1	Impurity 2
1	A	67.8	27.1	2.0	1.8	0.3
2	B	70.6	28.8	0.4	—	—
3	C	69.3	30.2	0.5	—	—

a) $NH_3/EO = 15$, WHSV 10 g $gcat^{-1}$ h^{-1}, reactor inlet temperature 343 K, reaction pressure 12 MPa. b) Catalyst A: La-ZSM-5 (commercially available) Al_2O_3 binder 30 wt %, B: La-ZSM-5 (commercially available) without binder, C: Binderless zeolite (NSC La-ZSM-5).

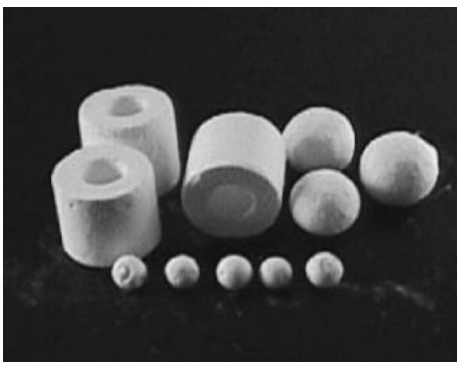

Fig. 12. Some examples of molded binderless zeolites.

To prevent the formation of impurities, a molded zeolite catalyst without a binder is required. Matsukata et al. have proposed a new zeolite synthetic method called "dry gel conversion."[56,57] Precursor gel containing a silica source, alkali, and a structure-directing agent (SDA) was contacted with high-temperature steam in an autoclave in order to crystallize to zeolite. This method was helpful to formulate the preparation of molded binderless zeolite. Shimizu et al. have also proposed solid state zeolite transformation method.[58,59]

We prepared molded binderless zeolite as follows.[60,61] Using the new solid-state crystallization (NSC) method, first, aluminum source, alkali, and SDA were impregnated into the molded silica support. Then, this precursor was dried and transferred into an autoclave. Finally, high-pressure and high-temperature steam was fed to the autoclave, and the precursor was crystallized to form molded zeolite. The obtained molded zeolite was robust enough for practical use.

As shown in Fig. 12, when molded silica of various shapes was used as a raw material, its whole body crystallized, maintaining its original shape. Figure 13 shows the XRD pattern of NSC ZSM-5. Sharp and strong diffraction lines, which were assigned to ZSM-5, showed good crystallinity. Figure 14 shows ^{29}Si and ^{27}Al MAS NMR spectra of NSC ZSM-5 and of commercially available ZSM-5. These spectrums show that NSC zeolite had few aluminum atoms out of lattice and Q^3-type silicon atoms. Figure 15 shows the morphology of NSC zeolite observed by FE-SEM. NSC ZSM-5 had sub-micrometer-sized minute crystals and good crystallinity. Figure 16 shows the morphology of molded binderless zeolite. For the same reason as discussed above about the clay catalyst, the catalyst diameter must be small. After crystallization, zeolite

beads were treated with ammonium nitrate to exchange sodium ion, and then they were calcined to decompose ammonium ion and SDA. Finally, proton of the zeolite was exchanged with La ion by a solid-state ion-exchange procedure. The catalytic performance of the NSC La-ZSM-5 catalyst was shown in Entry 3 of Table 13. Impurities were not detected. The NSC method can be applied to the synthesis of a zeolite other than ZSM-5, using various SDAs. Table 14 shows various crystallization products using various precursors and SDAs. In particular, β zeolite can be crystallized easily. Scale-up of the NSC method was comparatively easy, and large-scale industrialization of zeolite synthesis was accomplished.

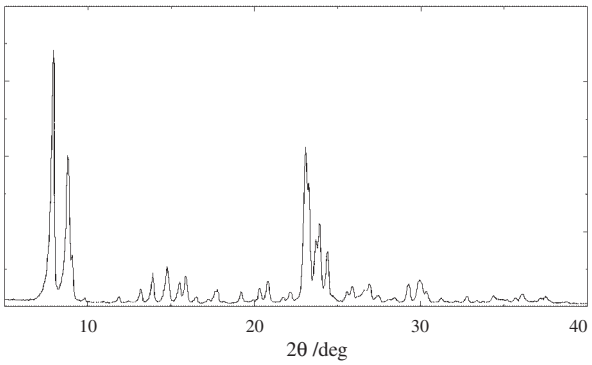

Fig. 13. XRD pattern of NSC zeolite (ZSM-5). X-ray: Cu Kα.

6. Process Development Using a Heterogeneous Catalyst

6.1 Adiabatic Reactor with Partially Vaporized Ammonia. The developed catalysts were calcined at temperatures above 800 K. Therefore, the catalysts have higher heat resistance than that of ion-exchange resin (allowable temperature limit: 393 K). Selectivities of both catalysts (clay and zeolite) were improved; thus, the reaction can be executed at high EO concentrations (i.e., low NH_3/EO molar ratio). In this case, the adiabatic temperature rise is a severe problem. The heat capacity (C_p) of the reaction mixture estimated using a simple mixing rule disagrees with an observed value (see Table 15).

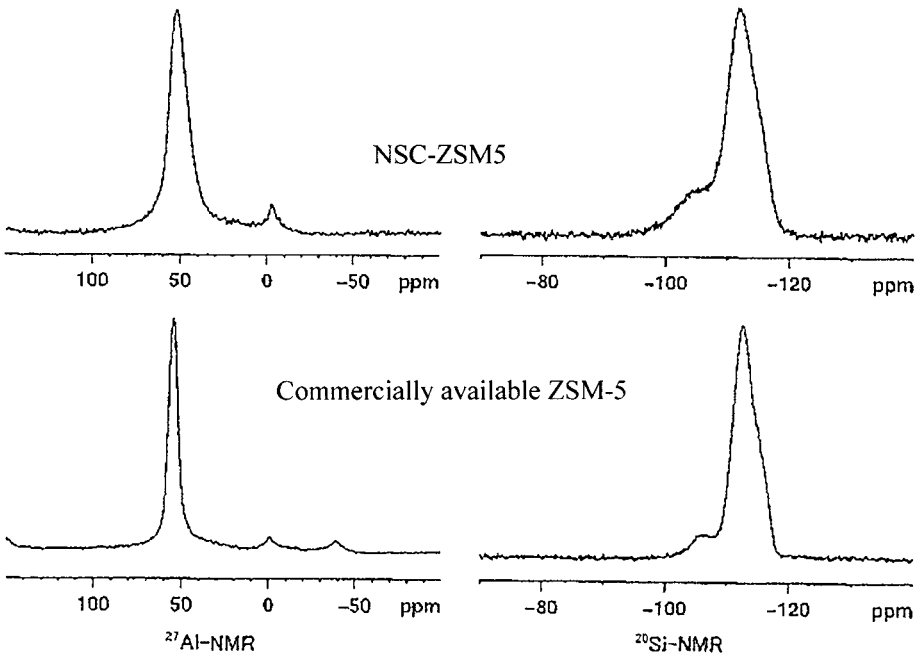

Fig. 14. ^{29}Si and ^{27}Al MAS NMR spectra of NSC zeolite (ZSM-5).

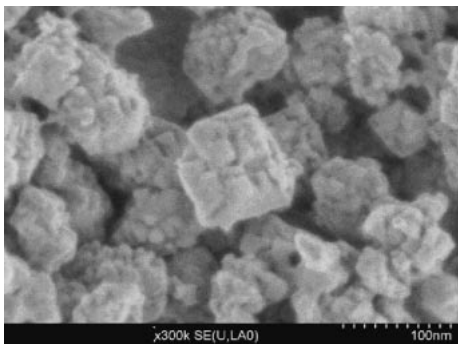

Fig. 15. Morphology of NSC zeolite (ZSM-5) crystal (FE-SEM).

Fig. 16. An example of a molded binderless zeolite (ZSM-5).

Table 14. Various Precursors and Crystallization Products of NSC Zeolite Method

SDA	Si/Na atomic ratio	Si/SDA molar ratio	Si/Al atomic ratio	Condition	Product
NPr_4OH	30	30	—	453 K, 8 h	Silicate-1
NPr_4OH	8	20	16	453 K, 8 h	ZSM-5
NBu_4OH	16	10	24	443 K, 32 h	ZSM-11
$MeNEt_3OH$	28	10	36	453 K, 48 h	ZSM-12
NEt_4OH	23	5	30	443 K, 20 h	β
NMe_4OH	20	5	—	443 K, 144 h	NU-1

Table 15. Effect of EO Concentration on Heat Capacity[a)]

NH_3/EO molar ratio	EO concentration /mol %	Reactor inlet–outlet temperature/K	Heat capacity/J g^{-1} deg^{-1}	
			Observed	Calculated value by mixing rule
NH_3	0	373.2	—	6.11
30.0	3.24	350.2–385.1	4.82	5.86
22.0	4.36	345.1–393.1	4.15	5.78
17.5	5.40	330.1–395.4	3.77	5.69
14.5	6.44	318.7–396.1	3.68	5.61

a) Reaction pressure: 12 MPa, heat capacity: average value of reactor inlet and outlet.

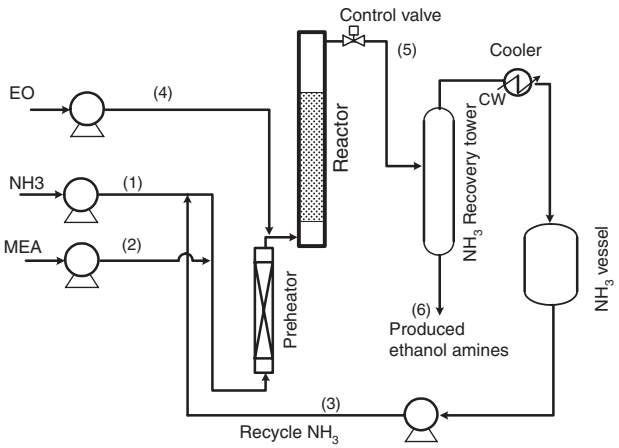

Fig. 17. Model flow sheet of a pilot plant. Reactor: 67 mm$^{\phi}$ 2000 mm^{L}, catalyst 4 to 6 L, with thermal insulation material wounded up. Heat liberation is compensated by heating.

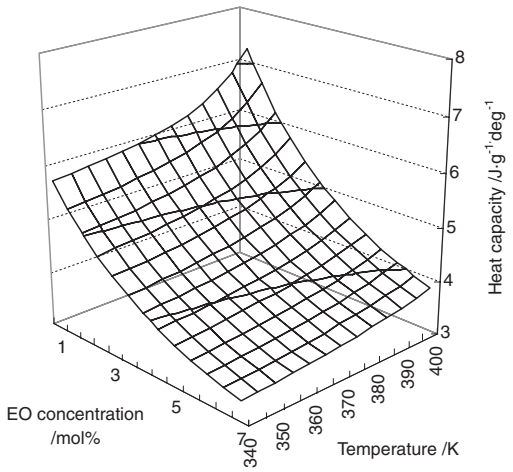

Fig. 18. Heat capacity of reaction mixture as a function of EO concentration and temperature, pressure: 12 MPa.

Vamling et al.[40] have reported an experimental equation of C_p (22) as a function of pressure (P) and temperature (T).

$$C_p = C_{p,a} + C_{p,b}/|(C_{p,c}{}^{(13\,\mathrm{MPa})} + \mathrm{d}C_{p,c}\mathrm{d}P(P - P_0) - T|, \quad (22)$$

P_0: $13 \cdot 10^6$ Pa; $C_{p,a}$, $C_{p,b}$, $C_{p,c}{}^{(13\,\mathrm{MPa})}$, $\mathrm{d}C_{p,c}\mathrm{d}P$: parameter. This equation does not involve an EO concentration term, but the EO concentration affects C_p considerably. The relationship between temperature rise and EO concentration was observed by using the pilot plant shown in Fig. 17. The reactor of this plant was highly insulated, and heat loss was compensated by heating to realize nearly adiabatic conditions. Heat capacity C_p is expressed as a function of EO concentration (C_E), pressure, and temperature (see Eq. 23):

$$C_p = C_{p,a} + a \cdot \exp(c \cdot C_E) + C_{p,b}/|(C_{p,c}{}^{(13\,\mathrm{MPa})} + b \cdot C_E + \mathrm{d}C_{p,c}\mathrm{d}P(P - P_0) - T|, \quad (23)$$

a, b, and c are additional parameters to Eq. 22 to explain the effects of EO concentration.

Figure 18 shows the heat capacity calculated following Eq. 23 at 12 MPa pressure. The heat capacity decreased markedly as the EO concentration increased. Figure 19 shows the adiabatic reaction temperature rise as a function of NH_3/EO molar ratio calculated using Eq. 23. The maximum temperature of the reactor was limited to under $\approx$420 K by-product qualities, such as coloring.

There are several means of suppressing temperature rise: (1) lower EO concentration in reaction mixture of reactor inlet, (2) use multiple reactors and split EO feed, and (3) use an heat-exchange-type reactor. These means have the strong disadvantage of increasing equipment cost.

We developed a process that can be operated in high EO concentrations and the temperature increase in the reaction mixture can be controlled.[62] A part of the ammonia is vaporized, and the reaction heat in an adiabatic reactor is eliminated by the heat of the ammonia vaporization. The reaction pressure

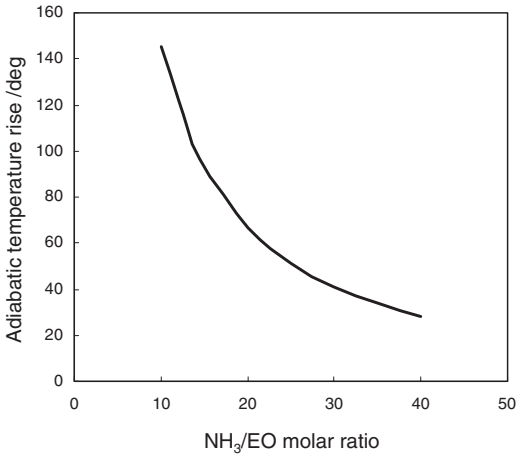

Fig. 19. Adiabatic reaction temperature rise as a function of NH_3/EO ratio.

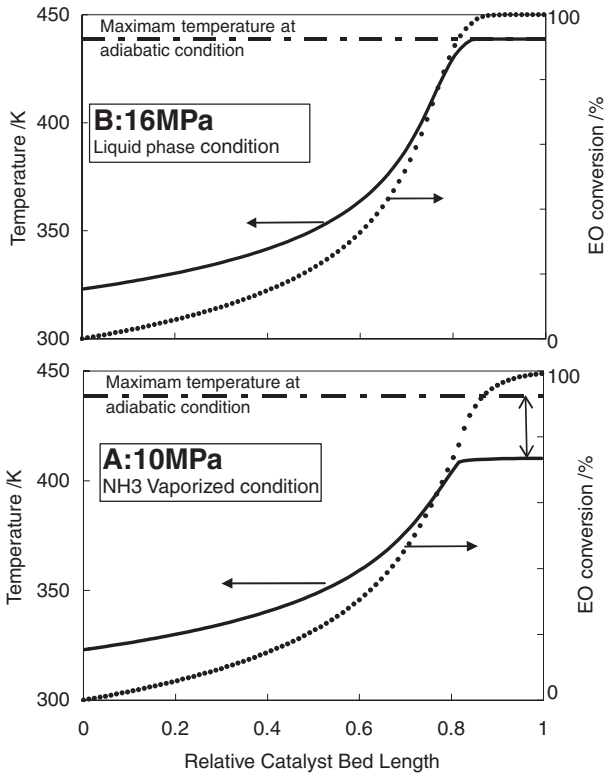

Fig. 20. Model temperature and EO conversion profile in catalyst bed. NH_3/EO molar ratio: 12, reactor inlet temperature: 323 K, reaction pressure: A: 10 MPa, B: 16 MPa, solid line: temperature profile (left axis), dotted line: EO conversion profile (right axis).

is controlled to reduce the boiling point of reaction mixture. Furthermore, even if the reaction heat rises as the reaction proceeds, ammonia vaporization by the reaction heat and the temperature rise of the catalyst bed is restrained.

Figure 20 shows the calculated profile of temperature and of EO conversion in the catalyst bed, at an NH_3/EO ratio of 12. In the case of B in Fig. 20, ammonia did not vaporize at the reaction pressure of 16 MPa, and the catalyst bed temperature increased with generated reaction heat, proportional to EO

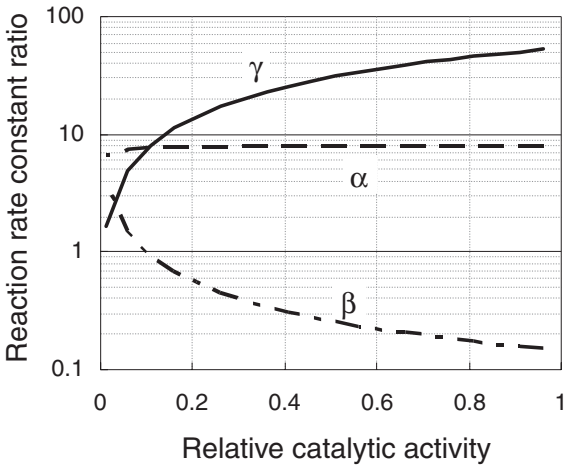

Fig. 21. Apparent selectivity change model along with deterioration. Plot of equation 19(α), 20(β), 21(γ) as a faction of relative k_{1c} calculated when $k_{1c}/k_O C_O = 50$, $\alpha_c = 8$, $\beta_c = 0.03$.

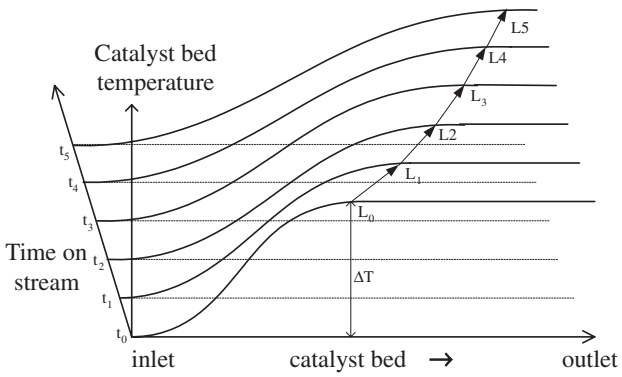

Fig. 22. Change of temperature profile along with catalyst deterioration.

conversion (e.g., 440 K at an inlet temperature of 323 K). In the case of A, at a reaction pressure of 10 MPa, vaporization of ammonia began when the temperature reached the boiling point of the reaction mixture, and temperature increased to about 410 K (30 K lower than A) very slowly.

6.2 Deterioration and Regeneration of Zeolite Catalyst. The data of the elapsed time of 24 h in Table 12 showed catalyst deterioration. Conversions of EO stayed at almost 100%, but DEA selectivity decreased. It became clear, by examining temperature distribution in the catalyst bed in detail, that there is activity deterioration from an entrance part. Decrease in activity may be caused by occlusion of micropores as a result of a zeolite catalyst. The reason why selectivity decreases along with activity deterioration is that non-catalytic reaction without selectivity becomes a dominant position in the activity-deteriorated catalyst bed. When intrinsic catalytic reaction rate constant k_{1c} in Eq. 21 becomes small, γ (DEA-selectivity indicator) becomes small (see Fig. 21). The same phenomenon occurs in the catalyst-unpacked part of the reactor[63] in the case of MEA recycle.

Development of a method to regenerate deactivated catalyst for practical use in a process using zeolite is extremely important. Figure 22 shows a change of model temperature profile in

an adiabatic reactor along with catalyst deterioration. Initially (t_0), the temperature increased at the entrance part of the reactor, because the catalyst had not yet deteriorated. The catalyst deteriorated from the entrance part as the reaction progresses ($t_0 \rightarrow t_5$), and the temperature of the deteriorated part of catalyst bed did not increase. Then, the peak of the temperature profile moved to the latter part ($L_0 \rightarrow L_5$) of the catalyst bed. It is necessary to regenerate a catalyst, because EO conversion and DEA selectivity decrease within a certain time. The deactivated catalyst did not discolor much and had the organic substance deposited in it, but the phenomenon did not involve coking, which is often the cause of catalyst deactivation. When coking occurs, the catalyst becomes black, and the organic substance becomes a carbon-like deposit. Such a substance can be removed only by oxidation at a temperature above 600 K. However, the deactivation of the catalyst in this reaction is not caused by coking; therefore, the catalyst can be regenerated by passing it through the catalyst rinse medium at a high temperature, which is more than the reaction temperature, to decompose or extract the deposited organic substance.[64] The selection of the medium is very important. When an inert gas, such as nitrogen, is used at temperatures higher than the reaction temperature, the organic substance becomes a carbon-like deposit. Solvent, supercritical fluid and high-density gas can be used. It is preferable not to bring in a new substance that is not used in the original process. Ammonia was used as a rinse medium was examined, because it is a stable substance used in the process. Ammonia reached its gas phase at a temperature higher than the reaction temperature. However, when it is pressurized at a high pressure, like the reaction pressure, its density is considerably larger, so it is an effective medium to regenerate the catalyst.[65]

Figure 23 shows the change in transition of the temperature peak in the catalyst bed along with the reaction and regeneration cycles. The catalyst activity was recovered from the deterioration in spite of repeating reaction and regeneration cycles. Figure 24 shows a model process flow sheet with a regeneration step. The reaction and regeneration steps were switched at intervals of several days. High boiling-point substances weeping from the catalyst were eliminated from the ammonia used in regeneration, and this recovered ammonia served as the raw material for the reaction. Plural reactors are necessary for concurrent reaction and regeneration. After regeneration, the flow channel is changed to the reaction system, and the reaction is restarted.

The developed process is made up from the following unique technologies. (1) zeolite catalyst, which is able to recognize the difference between DEA and TEA; (2) catalyst modification with rare earth element to improve activity drastically; (3) binderless molded zeolite; (4) catalyst regeneration using ammonia; and (5) reaction heat elimination using latent heat of vaporization in an adiabatic reactor.

The authors thank Mr. Shindo, Mr. Morishita, Mr. Arita, Mr. Takeda, Mr. Hashimoto, and Mr. Yokonuki for their continued support in catalyst and process development. The authors also thank the staff of the technical development and manufacture departments in the Chidori plant for their support in the industrialization of this process, and the staff of the catalyst manufacture department in the Himeji plant for the development and production of the commercial catalyst.

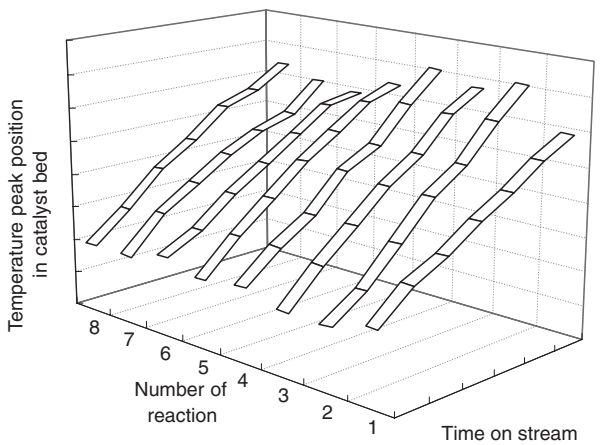

Fig. 23. Transition of temperature peak position with catalyst regeneration treated with ammonia at high temperature under high pressures.

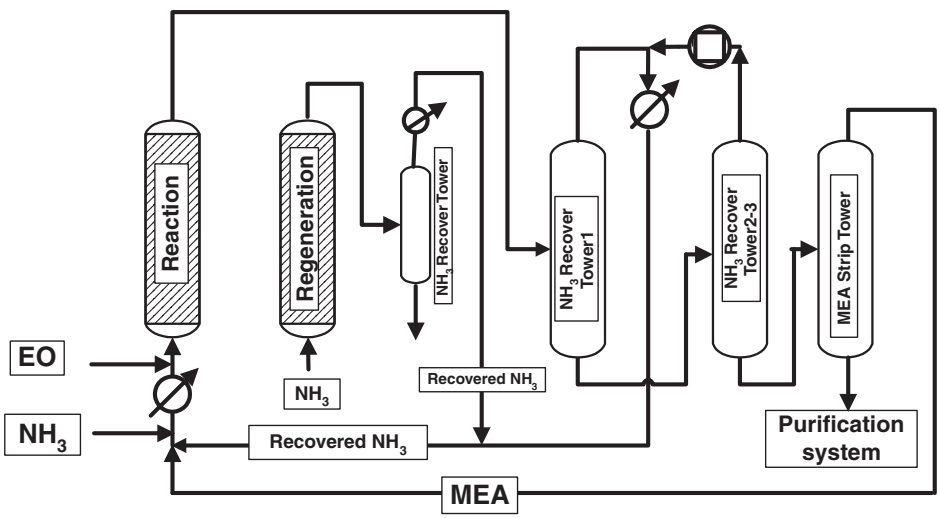

Fig. 24. Model process flow sheet. Reaction and NH_3 recovery system.

References

1 A. Wurtz, *Justus Liebigs Ann. Chem.* **1860**, *114*, 51; **1862**, *122*, 226.

2 L. Knorr, *Ber. Dtsch. Chem. Ges.* **1899**, *32*, 729.

3 M. R. Edens, J. F. Lochary, *Kirk-Othmer Encyclopedia of Chemical Technology*, John Wiley & Sons, New York, **1991**, Vol. 2, pp. 8–9.

4 G. Natta, E. Mantian, *J. Am. Chem. Soc.* **1952**, *74*, 3152.

5 P. Ferrero, F. Berbe, L. Flamme, *Bull. Soc. Chim. Belg.* **1947**, *56*, 349.

6 C. Potter, R. R. McLaughln, *Can. J. Res., Sect. B* **1947**, *25*, 405.

7 A. Lowe, D. Buttler, E. Meade, *Brit.* **1956**, *760*, 215.

8 M. Miki, T. Ito, M. Hatta, T. Okabe, *Yukagaku* **1966**, *15*, 215.

9 J. Przondo, Z. Kossonski, I. J. Onkowska, *Prizem. Chem.* **1974**, *53*, 757; Y. S. Ahn, T. Y. Lee, T. K. Chang, C. Chung, S. Ihm, *J. KIChE* **1980**, *18*, 393.

10 K. Park, T. Park, K. Byung, *Hwahak Konghak* **1985**, *23*, 409.

11 G. Schulz, W. Goetze, *Chem. Ing. Technol.* **1968**, *40*, 446.

12 R. Dahlinger, W. Goetze, G. Schulz, U. Sönksen, *DE-OS* **1972**, 1768335.

13 W. Goetze, P. Wolf, G. Schulz, H. Luedemann, U.S. Patent 3723530, **1973**.

14 M. J. Green, Eur. Pat. Appl. EP 171,893, **1986**.

15 Y. Watanabe, H. Sugawara, K. Suzuki, M. Matsumura, Jpn. Kokai Tokkyo Koho 94 199,746, **1994**; *Chem. Abstr.* **1994**, *121*, 300467.

16 Y. Watanabe, K. Suzuki, H. Sugawara, Jpn. Kokai Tokkyo Koho 94 247,909, **1994**; *Chem. Abstr.* **1994**, *122*, 30954.

17 Y. Watanabe, K. Suzuki, H. Sugawara, Jpn. Kokai Tokkyo Koho 94 247,910, **1994**; *Chem. Abstr.* **1994**, *122*, 30955.

18 Y. Watanabe, M. Matsumura, H. Sugawara, T. Okawa, K. Suzuki, Jpn. Kokai Tokkyo Koho 95 48,327, **1995**; *Chem. Abstr.* **1995**, *122*, 290331.

19 Y. Watanabe, M. Matsumura, H. Sugawara, T. Okawa, K. Suzuki, Jpn. Kokai Tokkyo Koho 95 70,004, **1995**; *Chem. Abstr.* **1995**, *122*, 290326.

20 Y. Watanabe, M. Matsumura, T. Okawa, K. Suzuki, Jpn. Kokai Tokkyo Koho 95 70,005, **1995**; *Chem. Abstr.* **1995**, *123*, 9065.

21 A. Moriya, H. T. Suneki, Jpn. Kokai Tokkyo Koho 95 126,228, **1995**; *Chem. Abstr.* **1995**, *123*, 9064.

22 A. Moriya, H. Tsuneki, Jpn. Kokai Tokkyo Koho 95 173,114, **1995**; *Chem. Abstr.* **1995**, *123*, 9064.

23 A. Moriya, H. Tsuneki, *Shokubai* **1996**, *38*, 91.

24 H. Tsuneki, *Shokubai* **1998**, *40*, 304; *Chem. Abstr.* **1998**, *129*, 244844.

25 H. Tsuneki, A. Moriya, H. Baba, Jpn. Kokai Tokkyo Koho 99 122,681, **1999**; *Chem. Abstr.* **1999**, *131*, 201526.

26 H. Tsuneki, M. Kirishiki, T. Oku, H. Shindo, Y. Hashimoto. H. Yokonuki, *Shokubai* **2004**, *43*, 84.

27 H. Tsuneki, *Recent Development of Zeolite Catalysts*, ed. by T. Tatsumi, Y. Nishimura, CMC Publishing, Tokyo, **2004**, p. 173.

28 H. Tsuneki, *Shokubai* **2005**, *47*, 196.

29 H. Hammer, W. Reutemann, Eur. Pat. Appl. EP 673,920, **1995**; U.S. Patent 5,545,757, **1996**.

30 S. B Willis, Jr., J. D. Henry, U.S. Patent 4,355,181, **1982**.

31 M. Ahmed, J. R. Nelson, C. A. Gibson, Eur. Pat. Appl. EP 99,416, **1984**; U.S. Patent 4,845,296, **1989**.

32 C. A. Gibson, M. Ahmed, J. R. Nelson, Eur. Pat. Appl. EP 100373, **1984**; U.S. Patent 4,847,418, **1989**.

33 A. F. A. Reynhart, U.S. Patent 2,186,392, **1938**.

34 B. J. G. Weibull, Swedish Patent 158,167, **1957**.

35 B. J. G. Weibull, L. U. F. Folke, S. O. Lindstrom, U.S. Patent 3697598, **1972**.

36 D. Kamemski, R. Boeva, N. Stoyanov, I. Taseva, *God. Vissh. Khim-Tekhnol. Inst., Burgas* **1984**, *19*, 53.

37 A. Stoyanov, R. Boeva, S. Kotov, *Zh. Prikl. Khim (Leningrad)* **1983**, *56*, 1966.

38 L. F. Johnson, Jr., L. Fred, U.S. Patent 4,438,281, **1984**.

39 J. N. Grice, J. F. Knifton, U.S. Patent 4,939,301, **1990**.

40 L. Vamling, L. Cider, *Ind. Eng. Chem. Prod. Res. Dev.* **1986**, *25*, 424.

41 U. Decker, J. Glietsch, I. Koch, K. Bergk, DD Patent, 298,633, **1992**; *Chem. Abstr.* **1992**, *117*, 5932.

42 U. Decker, J. Glietsch, I. Koch, K. Bergk, K. Heinz, I. Paleschke, W. Schwieger, DD Patent, 298,634, **1992**; *Chem. Abstr.* **1992**, *117*, 497.

43 U. Decker, J. Glietsch, I. Koch, K. Bergk, K. Heinz, I. Paleschke, W. Schwieger, DD Patent, 298,635, **1992**; *Chem. Abstr.* **1992**, *117*, 496.

44 U. Decker, J. Glietsch, I. Koch, K. Bergk, K. Heinz, I. Paleschke, W. Schwieger, DD Patent, 298,636, **1992**; *Chem. Abstr.* **1992**, *117*, 495.

45 Y. Izumi, K. Urabe, A. Onaka, *Shokubai* **1985**, *27*, 27.

46 E. W. Thiele, *Ind. Eng. Chem.* **1939**, *31*, 916.

47 A. Wheler, *Adv. Catal.* **1991**, *3*, 249.

48 S. M. Csicsery, *Pure Appl. Chem.* **1986**, *58*, 841.

49 C. Jia, P. Beaunier, P. Massiani, *Microporous Mater.* **1998**, *24*, 69.

50 M. Rauscher, K. Kesore, R. Mönnig, W. Schwieger, A. Tißler, T. Turek, *Appl. Catal., A* **1999**, *184*, 249.

51 M. Kirishiki, H. Tsuneki, F. Morishita, M. Urano, Jpn. Kokai Tokkyo Koho 2002 028,492, **2002**; *Chem. Abstr.* **2002**, *136*, 120219.

52 N. Saito, *SPring8 Report*, **2004**, A0788-RI-TU BL19B2.

53 S. J. Washington, T. F. Grant, U.S. Patent 5,334,763, **1994**.

54 S. J. Washington, T. F. Grant, WO 9,424,089, **1994**.

55 D. M. Nygaard, R. M. Diguilio, U.S. Patent, 6,063,965, **2000**.

56 P. R. H. P. Rao, M. Matsukata, *Chem. Commun.* **1996**, 1441.

57 M. Matsukata, N. Nishiyama, K. Ueyama, *Microporous Mater.* **1996**, *7*, 109.

58 S. Shimizu, Y. Kiyozumi, F. Mizukami, R. M. Mihayli, H. K. Beyer, *Adv. Mater.* **1996**, *8*, 759.

59 S. Shimizu, Y. Kiyozumi, F. Mizukami, *Chem. Lett.* **1996**, 403.

60 T. Oku, H. Tsuneki, 86th CATSJ Meeting, **2000**, Abstr., No. 4E19.

61 T. Oku, H. Tsuneki, Jpn. Kokai Tokkyo Koho 2001 58,817, **2001**.

62 H. Tsuneki, A. Moriya, Jpn. Kokai Tokkyo Koho 97 52,869, **1997**; *Chem. Abstr.* **1997**, *126*, 263841.

63 H. Tsuneki, Jpn. Kokai Tokkyo Koho 2000 288,378, **2000**; *Chem. Abstr.* **2000**, *133*, 298003.

64 H. Tsuneki, M. Kirishiki, Y. Arita, Y. Hashimoto, T. Oku, H. Shindo, M. Urano, Jpn. Kokai Tokkyo Koho 2001 151,740, **2001**; *Chem. Abstr.* **2001**, *135*, 5375.

65 H. Tsuneki, T. Oku, M. Urano, F. Morishita, Jpn. Kokai Tokkyo Koho 2001 314,771, **2001**; *Chem. Abstr.* **2001**, *135*, 349268.

Hideaki Tsuneki was born in 1953 in Fukushima, Japan. After graduating Tokyo Institute of Technology in 1976, he entered the graduate school of the same university. After he received a master's degree from the Tokyo Institute of Technology in 1978, he joined Nippon Shokubai Chemical Industry. He was engaged in studies on methacrylic acid synthesis catalyst in 1978 to 1985, in development of ethyleneimine production process and catalyst from 1985 to 1990, and development of 2-aminoethanol and 2,2′-iminodiethanol production process and catalyst from 1991 to 2003. In 1992 he received the 41st Chemical Society of Japan Award for Technical development, and the Catalyst Society of Japan Award in Technical Division. Now, he is a Senior Technical Adviser of R&D division and a General Manager of Strategic Technology Research Center of Nippon Shokubai Co., Ltd.

Masaru Kirishiki was born in 1963 in Ishikawa, Japan. After graduating Toyama University in 1986, he entered the graduate school of the same university. After he received a master's degree from Toyama University in 1988, he joined Nippon Shokubai Chemical Industry. He was engaged in studies on acrylic acid synthesis catalyst from 1988 to 1990, in development of secondary alcohol ethoxide production process and catalyst from 1990 to 1999 and development of dimethyl carbonate production process and catalyst in 1992 to 1994, and development of 2,2′-iminodiethanol production process and catalyst from 1999 to 2003. Now he is a Research Manager of Strategic Technology Research Center of Nippon Shokubai Co., Ltd.

Tomoharu Oku was born in 1966 in Kitakyushu, Japan. After graduating Tokyo University of Science in 1989, he entered the Interdisciplinary Graduate School of Science and Engineering at the Tokyo Institute of Technology (Titech). After he received a master's degree from Titech, he joined Nippon Shokubai Co., Ltd. in 1992. He was engaged in studies on metal catalysts for chemical synthesis from 1992 to 1994, and various solid acid–base catalyses in supercritical fluids from 1994 to 1997, and solid-phase synthesis of zeolite in 1998, and development of the 2,2′-iminodiethanol production process and catalyst from 1999 to 2000. In addition he joined on temporary to the NEDO's project of "Development of Technology to Reduce the Burden on the Environment Using Supercritical Fluid" in Titech from 2000 to 2002. Now he is a Research Manager of Strategic Technology Research Center of Nippon Shokubai Co., Ltd.